

Lineshape of the Higgs boson in future lepton colliders^{*}

S. Jadach^a and R.A. Kycia^b

^a*The Henryk Niewodniczański Institute of Nuclear Physics,
Polish Academy of Sciences,
ul. Radzikowskiego 152, 31-342 Kraków, Poland*

^b*T. Kościuszko Cracow University of Technology,
Faculty of Physics, Mathematics and Computer Science,
ul. Warszawska 24, Kraków, 31-155, Poland*

Abstract

The effect of the photon emission (bremsstrahlung) in the cross section of the process of direct production of the Higgs boson in the future high luminosity electron and muon colliders is calculated. It was found that cross section at the top of the Higgs boson resonance peak is reduced by factor 0.347 for the electron collider and 0.548 for the muon collider. Machine spread of the centre of the mass energy of 4.2MeV (equal to the Higgs width) would reduce peak cross section further, by factor 0.170 and 0.256 (QED and energy spread) for electron and muon beams respectively. Possible uncertainties in the resummed QED calculations are discussed. Numerical results for the lineshape cross section including QED and many values of the machine energy spread are provided.

Keywords: QCD, the Higgs boson cross section, energy scan, beam spread, initial radiation state.

IFJPAN-IV-2015-3

^{*}This work is partly supported by the Polish National Science Centre grant UMO-2012/04/M/ST2/00240.

Contents

1	Introduction	2
2	QED initial state radiation formulas	2
3	Machine energy spread	4
4	Numerical results for electron-positron colliders	4
5	Numerical results for muon colliders	6
6	Summary	7
A	Non-uniqueness of the Breit-Wigner formula	8
B	Approximate formulas for QED ISR	8

1 Introduction

Observation of the Higgs particle at CERN [1–3] has opened the new era of precise study of its properties. Once its mass is known, one may reconsider a possibility of its direct observation in the lepton annihilation $e^-e^+ \rightarrow H$ or $\mu^-\mu^+ \rightarrow H$, at future electron colliders or dedicated muon collider. Due to extremely small coupling of the Higgs boson to electron, it seems at first sight that its direct production in the electron collider is just hopeless. However, in the Future Circular Collider with e^\pm beams (FCCee) considered at CERN featuring very high luminosity, this process would in principle be observable, provided one could eliminate copious background processes. On the other hand, stronger coupling of Higgs to muons puts dedicated muon collider into a definite advantage, provided decent luminosity and small beam energy spread are achieved. In either case, machine energy spread and an additional smearing of the beam energy due to QED bremsstrahlung are major points in the feasibility studies of these projects. This is why the present study was undertaken. The influence of the beam energy spread on observability of the direct Higgs observation in FCCee collider was already discussed at the 8th FCC-ee Physics Workshop [4]. In this work we shall concentrate mainly on calculating effects due to initial state radiation of multiple photons. This will be done exploiting past experience in calculating very precisely similar QED effect for the Z boson productions at LEP experiments, for instance in ref. [5]. Similar analysis of the initial state QED corrections, taking into account the machine energy spread, for $\mu^-\mu^+ \rightarrow H$ process can be also found¹ in refs. [6] and [7].

The paper is organized as follows: After defining the Born cross section for the Higgs process production in the lepton annihilation, we will discuss the effect of the initial state radiation (ISR) corrections. We shall discuss theoretical uncertainties in the evaluation of this QED effect, presenting numerical results for three different QED ISR formulas, of the varying sophistication level. The effect of the machine energy spread in the cross section will be added in the discussion, presenting numerical results for several values of such a spread. Finally the analogous effects in planned muon colliders will be discussed and numerical results will be presented.

2 QED initial state radiation formulas

Born cross section for the Higgs particle production in e^\pm collider is given by the (relativistic [8]) Breit-Wigner (B-W) formula [5]

$$\sigma_B(s) = \frac{4\pi B_{ee}\Gamma_H^2}{(s - M_H^2)^2 + \Gamma_H^2 M_H^2}, \quad (2.1)$$

where $M_H = 125.7$ GeV and $\Gamma_H = 4.2$ MeV according to refs. [9, 10]. The branching ratio of $e^+e^- \rightarrow H$ is $B_{ee} = 5.3 \cdot 10^{-9}$. The electron and muon branching ratios are related by the factor m_μ^2/m_e^2 , thus the above result can be obtained from $B_{\mu\mu} = 2.19 \cdot 10^{-4}$, see also

¹We thank M. Greco and S. Dittmaier for bringing these works to our attention.

refs. [9, 10]. There are variants of the B-W formulas with the s -dependent width, but for the narrow resonance like Higgs they differ negligibly from the above, see more discussion in the Appendix A.

The initial state radiation correction to this process was calculated using formulas of ref. [5] for Z boson production². The entire initial-state $\mathcal{O}(\alpha^2)_{\text{prag}}$ formula of ref. [5] integrated cross section reads:

$$\sigma_I(s) = \int_0^1 dv \rho_I(v) \sigma_B(s(1-v)), \quad (2.2)$$

$$\rho_I(v) = e^{\delta_{YFS}} F(\gamma) \gamma v^{\gamma-1} \{d_s + \Delta_H(v)\},$$

where

I	d_s	$\Delta_H(v)$
(a)	1	0
(b)	$1 + \frac{\gamma}{2} + A \frac{\alpha}{\pi}$	$v \left(-1 + \frac{1}{2}\right)$
(c)	$1 + \frac{\gamma}{2} + \frac{\gamma^2}{8} + A \frac{\alpha}{\pi}$	$v \left(-1 + \frac{1}{2}\right) + \gamma \left[-\frac{v}{2} - \frac{1+3(1-v)^2}{8} \ln(1-v)\right]$

(2.3)

and

$$\delta_{YFS} = \frac{\gamma}{4} + \frac{\alpha}{\pi} \left(-\frac{1}{2} + \frac{\pi^3}{3}\right), \quad (2.4)$$

$$\gamma = 2 \frac{\alpha}{\pi} \left(\ln \frac{s}{m_e^2} - 1\right), \quad F(\gamma) = \frac{\exp(-C\gamma)}{\Gamma(1+\gamma)}.$$

Here, α is the QED coupling constant, m_e the electron mass and C is the Euler-Mascheroni constant. In case of the muon beams m_e in γ is replaced by m_μ and B_{ee} by $B_{\mu\mu}$.

Zero spin nature of the Higgs boson instead of spin one of Z counts negligibly in the QED ISR effects, simply because deformation of the resonance curve is mainly due to soft photons. The constant A which is responsible for the above spin difference is of order $\frac{\alpha}{\pi} \simeq 1/400$ without any logarithmic enhancement. It is influencing mainly an overall normalization – hence at the precision level we are aiming at, it can be safely set to zero³

On the other hand soft photon exponentiation/resummation in eq. (2.2) is critical and mandatory. The formula of eq. (2.2) comes from standard diagrammatic perturbative QED calculations including Yennie-Frautschi-Suura (YFS) exponentiation, see ref. [5] and was originally introduced for the purpose of the algebraic validation of the Monte Carlo program YFS2 of ref. [11]. Later on it was discussed and used in many papers, see for instance refs. [5, 12–15] and the references therein.

Three variants (for $I = (a), (b)$ or (c)) of the ISR formula in eq. (2.2) correspond to the increasing sophistication (perturbative order) of the non-soft collinear radiative corrections. Change of the type of ISR formula will be used to estimate uncertainty due to unknown/neglected QED higher orders.

²See eq. (202) therein.

³ Constant A is also set to zero in ref. [7], while in ref. [6] vertex and real-soft contributions are provided, but non-logarithmic constant A was explicitly obtained.

E	σ_B	$\sigma_{(a)}$	$\sigma_{(b)}$	$\sigma_{(c)}$	$\frac{\sigma_{(a)}}{\sigma_B}$	$\frac{\sigma_{(b)}}{\sigma_B}$	$\frac{\sigma_{(c)}}{\sigma_B}$
M_H	1.6413	0.5398	0.5693	0.5701	0.328	0.346	0.347
$M_H + \Gamma_H$	0.3283	0.1846	0.195	0.1949	0.562	0.594	0.593
$M_H - \Gamma_H$	0.3283	0.1073	0.1134	0.1133	0.326	0.345	0.345

Table 1: Born cross sections (in fb) of eq. (2.1) and three variants of the ISR-corrected cross sections of eq. (2.2) for three values of $\sqrt{s} = E = M_H = 125.7$ GeV and $E = M_H \pm \Gamma_H$ in the electron-positron collider. The integration error is below $0.0005fb$.

3 Machine energy spread

In real accelerator experiments the beam is not monoenergetic, i.e., centre-of-mass energy $E = \sqrt{s}$ has spread δ around the centre value $E_0 = \sqrt{s_0}$ of the beam energy. The distribution of E is usually well approximated by the following Gaussian distribution

$$G(E - E_0; \delta) = \frac{1}{\delta\sqrt{2\pi}} e^{-\frac{(E-E_0)^2}{2\delta^2}}. \quad (3.1)$$

In case of no QED effects, the Born cross section (2.1) gets simply convoluted with the energy spectrum of eq. (3.1):

$$\sigma_B^{conv}(E; \delta) = \int dE' \sigma_B(E') G(E' - E; \delta). \quad (3.2)$$

Once QED bremsstrahlung is switched on, the following double convolution provides realistic experimental cross section:

$$\begin{aligned} \sigma_I^{conv}(E; \delta) &= \int dE' \sigma_I(E') G(E' - E; \delta) \\ &= \int dE' \int_0^1 dv \frac{1}{\delta\sqrt{2\pi}} e^{-\frac{(E'-E)^2}{2\delta^2}} \rho_I(v) \sigma_B(E'^2(1-v)), \end{aligned} \quad (3.3)$$

for three variants, $I = (a), (b), (c)$ of the radiative function (2.2).

Because of rapid decrease of the Gaussian distribution for large arguments, the energy integration range will be restricted to $E - 10\delta \leq E' \leq E + 10\delta$ without any loss of the calculation reliability. The numerical integrations in one and two dimensions require a little bit of care, because of strongly singular integrands. The adaptive integration library functions of ROOT library [16] were used. All results were also cross-checked using FOAM adaptive Monte-Carlo simulator/integrator of [17–19]⁴.

4 Numerical results for electron-positron colliders

The Born cross sections and results from three variants of the ISR formula of eq. (2.2) are presented in Fig. 1. The case $\sigma_{(b)}$ and $\sigma_{(c)}$ are almost indistinguishable. In addition,

⁴ Integration errors were also taken from FOAM, as they are more reliable.

E	σ_B	(1)	(2)	(3)	$\frac{(1)}{\sigma_B}$	$\frac{(2)}{\sigma_B}$	$\frac{(3)}{\sigma_B}$
M_H	1.6413	0.5701	0.2795	0.1825	0.347	0.170	0.111
$M_H + \Gamma_H$	0.3283	0.1950	0.2323	0.1753	0.594	0.708	0.534
$M_H - \Gamma_H$	0.3283	0.1133	0.1865	0.155	0.345	0.568	0.472

Table 2: Cross section of the direct Higgs production process in the electro-positron collider including effect of ISR type (c) and the machine energy spread. No energy spread is in $\sigma_{(1)}$, while $\sigma_{(2)}$ and $\sigma_{(3)}$ include ISR and energy spread $\delta = 4.2 \text{ MeV}$ and $\delta = 8.0 \text{ MeV}$ according to eq. (3.3). Reference Born cross section σ_B is also included and the ratios with respect to Born are also provided. The integration error is below $0.0005fb$.

Tab. 1 presents the same results for the energy at the peak $E = M_H$ and near the peak $E = M_H \pm \Gamma_H$ with the 4-digit precision. The QED uncertainty from unaccounted QED higher orders can be estimated from Tab. 1 looking into differences between ISR type $I = (c)$ and $I = (b)$. It is below 0.3% and is compatible with the estimate of neglected A in eq. (2.2) (it is also comparable to the numerical integration error). From now on we shall use ISR formula for $I = (c)$ only.

The introductory exercise on the machine energy spread is shown in Fig. 2 where Higgs production cross section in the electron-positron collider is plotted without energy spread (Born) and for several values of the machine energy spread $\delta = 4.2, 8, 15, 30, 100\text{MeV}$. The QED ISR effect is not yet included.

On the other hand Fig. 3 shows our most interesting result, that is Higgs production cross section in the electron-positron collider including both QED ISR effect according to eq. (3.3) for ISR type (c) and for several examples of the machine energy spread parameter $\delta = 4.2, 8, 15, 30, 100\text{MeV}$.

In Fig. 4 we plot again the same Higgs production cross section in the electron-positron collider including both QED ISR effect and machine energy spread in the narrower energy range and for the energy spread parameter $\delta = 4.2\text{MeV}$ which is ambitiously aimed at the FCCee collider, and also for more realistic $\delta = 8.0\text{MeV}$. The ratio of cross section with respect to Born is also shown in the lower plot there.

The same results as in Fig. 4 are also shown in Tab. 2 for three values of the energy, at the resonance peak $E = M_H$ and near the peak $E = M_H \pm \Gamma_H$, with the 4-digit precision. As we see there, the combined reduction of the Higgs production process at the resonance peak due to QED effect is 0.347 and goes down to 0.170 for the machine energy spread equal to Higgs width $\sim 4.2\text{MeV}$.

The suppression factor of the peak cross section due to QED ISR can be also quite well reproduced, and in this way cross checked, with very simple approximate calculation presented in Appendix B. This approximation works even better in case of the weaker ISR effect for muon beams.

The above results can be used as an input for further studies of the practical observability of the Higgs resonant cross section in the future electron-positron colliders.

In the above numerical exercises we have used discrete values of the machine energy spread δ . In Fig. 5 we also show the continuous dependence on δ of the Higgs production

	σ_B	(1)	(2)	(3)	$\frac{(1)}{\sigma_B}$	$\frac{(2)}{\sigma_B}$	$\frac{(3)}{\sigma_B}$
E_0	67.8198	37.14	17.34	11.06	0.548	0.256	0.163
$E_0 + \Gamma_H$	13.5636	10.36	13.62	10.32	0.764	1.004	0.761
$E_0 - \Gamma_H$	13.5643	7.40	11.95	9.62	0.546	0.881	0.709

Table 3: Cross section of the direct Higgs production process in the $\mu^+\mu^-$ collider including effect of ISR type (c) and the machine energy spread. The same values of the energy spread δ an energy E are used as in Tab.2. The Monte Carlo integration error is below $0.03pb$.

process at the resonance peak, $E = M_H$, divided by the Born cross section, both for QED ISR switched on and off. More precisely, we are plotting there the following two ratios

$$\frac{\sigma_B^{conv}(M_H, \delta)}{\sigma_B(M_H)} \quad \text{and} \quad \frac{\sigma_{(c)}^{conv}(M_H, \delta)}{\sigma_B(M_H)}, \quad (4.1)$$

for ISR off and on respectively.

One could easily expand the above numerical exercises to more values in the 2-dimensional space of the energy E and machine energy spread δ , but we think that numerical results collected above are complete enough and can serve as a reliable starting point for all studies of the Higgs resonance observability in the future electron-positron colliders.

It is worth to pointing out that because of the normalization of convolution as a function of δ at $E = M_H$ to unity we can construct the following quantity that is close unity when δ/Γ_H is not too big. In Fig. 7 the following quantity

$$R_V(E, \delta) = \frac{\sigma_B^{conv}(E, \delta)}{\sigma_B(E)} \left(\frac{\sigma_{(c)}^{conv}(E, \delta)}{\sigma_{(c)}^{conv}(E, 0)} \right)^{-1} \quad (4.2)$$

is plotted. If $R_V(E, \delta) \simeq 1$ then double convolution can be replaced by the following handy approximation

$$\sigma_{(c)}^{conv}(E, \delta) \simeq \sigma_{(c)}^{conv}(E, 0) \frac{\sigma_B^{conv}(E, \delta)}{\sigma_B(E)}.$$

As seen in Fig. 7 the above approximation for $E = M_H$ works reasonably, within 10% for $\delta \leq \Gamma_H$, but its validity deteriorates significantly for $\delta > \Gamma_H$ and in such a case numerical double convolution is unavoidable.

5 Numerical results for muon colliders

The calculations of the previous section can be easily extended to the case of muon collider, in the so-called Higgs factories (for overview see, e.g., [20]), by means of replacing m_e with m_μ and B_{ee} with $B_{\mu\mu}$ in the equations of section 2 (see also [6] or [7]). This kind of colliders will produce clean sample of Higgs boson without much background and therefore would

allow to measure Higgs mass and its properties very precisely. Our analysis is vital in view of MAP (Muon Accelerator Program) [20] at Fermilab and the new ideas of producing muon monochromatic beams, that would allow to limit the major obstacle, the machine energy spread.

Thanks to much higher branching ratio for the Higgs to muon pair, the production cross section for the $\mu^+\mu^- \rightarrow H$ is much higher. Also, QED effects for muon collider are roughly factor 2 weaker, simply because for muon beams at the Higgs peak $\gamma = 0.0611$, as compared to $\gamma = 0.1106$ for electron beams.

Numerical results for muon collider are presented in Fig. 6 and Tab. 3, and correspond to Higgs production cross section dependence on energy E and machine energy spread δ shown in Fig. 4 and in Tab. 2. As seen in this table, reduction factor of the cross section at the resonance peak due to QED ISR is now only 0.548. For the machine energy spread $\delta = 8\text{MeV}$ it deteriorates down to 0.162 (which is accidentally comparable to electron collider case with $\delta = 4\text{MeV}$) and for $\delta = 4.2\text{MeV}$ it is equal 0.279⁵.

6 Summary

It was analysed numerically what is the influence of the QED ISR and machine energy spread on the the resonant Higgs boson production cross section, the so called Higgs line-shape, in the process $e^+e^- \rightarrow H$ and $\mu^+\mu^- \rightarrow H$.

It was found that for electron collider the QED ISR reduces by itself peak cross section by factor 0.338. The QED higher order uncertainty of this results was estimated to be below 0.3%. The proper double convolution of the QED radiative spectrum with the machine energy spread was performed and doubly cross-checked. For instance machine energy spread of the same size as Higgs width ($\delta \simeq 4\text{MeV}$) reduces Higgs production cross section further down to $0.172\sigma_B$. These results are compatible (albeit slightly different) from these in the preliminary analysis shown at the recent FCCee workshop, see [4]. It forms a solid basis for any analysis of the observability of the Higgs resonant cross section in the future e^+e^- colliders.

The same analysis was also repeated for the muon colliders, where the reduction factor due to QED ISR at the peak position was found to be 0.548 and, for instance, it gets reduced further down to 0.162 for the energy beam spread being twice the Higgs width.

⁵This agrees only rather crudely with 0.25 result in ref. [7] for $\delta = 4\text{MeV}$, obtained from approximate analytical formula.

A Non-uniqueness of the Breit-Wigner formula

In this short Appendix we want to comment on the issue of the form of the non-uniqueness of the Breit-Wigner formula (2.1) and we shall show that for extremely narrow Higgs boson resonance this non-uniqueness is numerically completely irrelevant.

The literature on this question is numerous, for instance in the context of the precision measurements of the Z and W boson production and decay the reader may consult refs. [21–24]. In particular the use of the complex energy poles of the propagator of virtual particles as a natural solution was advocated, see ref. [24].

Following ref. [21] (eqs. (1.6) through (1.9)), the Born term corresponding to (2.1) is

$$\sigma_B(s) \sim \frac{s}{(s - M_H^2)^2 + G^2}. \quad (\text{A.1})$$

In case of constant width $G = M_H^2 \gamma_H = 527.94$ where $\gamma_H = \frac{\Gamma_H}{M_H} = 3.34 \cdot 10^{-5}$, while for the s dependent one we have $G = G(s) = s\gamma_H$. The maximum of the cross section is at

$$\sqrt{s_0} = E_0 = M_H(1 + \gamma_H^2)^{1/4} \simeq M_H(1 + \frac{\gamma_H^2}{4}) = 125.700000035 \text{ GeV} \quad (\text{A.2})$$

for the fixed width and

$$E_0 = M_H(1 + \gamma_H^2)^{-1/4} \simeq M_H(1 - \frac{\gamma_H^2}{4}) = 125.69999996 \text{ GeV} \quad (\text{A.3})$$

for s -dependent width. The difference between E_0 in the above two cases may be regarded as 7×10^{-8} GeV. To our knowledge it is practically impossible to achieve energy resolution in accelerators of that order of magnitude.

Finally, the formula with the so-called running width (for different variants of Breit-Wigner see, e.g., [25] and references therein) reads

$$\sigma_B(s) \sim \frac{1}{(s - M_H^2)^2 + G^2}, \quad (\text{A.4})$$

where $G = s\gamma_H$. The maximum of the cross section is at

$$\sqrt{s_H} = \frac{M_H}{\sqrt{1 + \gamma_H^2}} \simeq M_H(1 - \frac{\gamma_H^2}{2}), \quad (\text{A.5})$$

which, as above, is beyond measurability in any future accelerator experiment.

B Approximate formulas for QED ISR

Starting from eq. (2.2) we are going to provide a very simple approximate formula that allows to estimate the suppression factor of the peak cross section at $s = M_H^2$ due to QED ISR corrections, thus providing quick/easy cross-check of more sophisticated numerical calculations.

In the most simplified soft photon approximation ISR formula of eq. (2.2) at $E = M_H$ reads

$$\sigma(M_H) \approx \int_0^1 \gamma v^{\gamma-1} \sigma_B(M_H^2(1-v)) dv. \quad (\text{B.1})$$

It is well known fact that Breit-Wigner profile drop sharply around $|s - M_H^2| = \Gamma_H^2$ and one may therefore approximate it by the following rectangular shape

$$\sigma_B(s) \simeq \sigma_B(M_H^2) \theta(|s - M_H^2| < \Gamma_H^2),$$

which translates into $v \leq \Gamma_H/M_H$ integration limit. As a result we obtain the following approximate suppression factor for ISR corrections

$$r_{ISR} = \frac{\sigma_I(M_H^2)}{\sigma_B(M_H^2)} \simeq \frac{1}{\sigma_B(M_H^2)} \int_0^{\frac{\Gamma_H}{M_H}} \gamma v^{\gamma-1} \sigma_B(M_H^2) dv = \left(\frac{\Gamma_H}{M_H} \right)^\gamma \quad (\text{B.2})$$

For e^+e^- colliders with $\gamma = 0.1106$ the ISR suppression factor is then estimated to be

$$r_{ISR} = 0.3199. \quad (\text{B.3})$$

This agrees reasonably well with the exact ISR factor of 0.347, seen in Tab. 1. The relative error of the approximate formula is about 8%⁶. For $\mu^+\mu^-$ collider with smaller $\gamma = 0.0611$ approximate ISR suppression factor

$$r_{ISR} = 0.5329, \quad (\text{B.4})$$

is obtained, to be compared with the corresponding value of 0.548 in Tab. 3. The relative error of the approximate formula is now merely 3%.

References

- [1] CMS, S. Chatrchyan *et al.*, Physics Letters B **716**, 30 (2012).
- [2] ATLAS, G. Aad *et al.*, Physics Letters B **716**, 1 (2012).
- [3] CMS, S. Chatrchyan *et al.*, JHEP **1306**, 081 (2013), 1303.4571.
- [4] D. d’Enterria, G. Wojcik, and R. Aleksan, Presentation at 8 FCC-ee Physics Workshop (2014).
- [5] S. Jadach, B. F. L. Ward, and Z. Was, Phys. Rev. **D63**, 113009 (2001), hep-ph/0006359.
- [6] S. Dittmaier and A. Kaiser, Phys. Rev. **D65**, 113003 (2002), hep-ph/0203120.

⁶ Sometimes one expands further $r_{ISR} \simeq 1 - \gamma \ln(\Gamma_H/M_H)$ but this makes sense only for $r_{ISR} > 0.5$, which is not our case.

- [7] M. Greco, (2015), 1503.05046.
- [8] Peskin, Michael E. and Schroeder, Dan V., *An Introduction To Quantum Field Theory* (Westview Press, 1995).
- [9] Beringer, J. et al., *Status of Higgs Boson Physics* (, 2012 and 2013 update for the 2014 edition).
- [10] K.A. Olive et al., *Status of Higgs Boson Physics* (, 2014).
- [11] S. Jadach and B. F. L. Ward, Comput. Phys. Commun. **56**, 351 (1990).
- [12] S. Jadach, M. Skrzypek, and M. Martinez, Physics Letters **B280**, 129 (1992).
- [13] S. Jadach, B. Pietrzyk, and M. Skrzypek, Physics Letters **B456**, 77 (1999).
- [14] S. Jadach, M. Skrzypek, and B. Ward, Physics Letters **B257**, 173 (1991).
- [15] M. Skrzypek, S. Jadach, M. Martinez, W. Płaczek, and Z. Was, Physics Letters **B372**, 289 (1996).
- [16] I. Antcheva *et al.*, Computer Physics Communications **180**, 2499 (2009), 40 YEARS OF CPC: A celebratory issue focused on quality software for high performance, grid and novel computing architectures.
- [17] S. Jadach, Comput. Phys. Commun. **130**, 244 (2000), physics/9910004.
- [18] S. Jadach, Comput. Phys. Commun. **152**, 55 (2003), physics/0203033.
- [19] M. Slawinska and S. Jadach, Comput. Phys. Commun. **182**, 748 (2011), 1006.5633.
- [20] MAP, MICE, D. M. Kaplan, EPJ Web Conf. **95**, 03019 (2015), 1412.3487.
- [21] D. Y. Bardin, A. Leike, T. Riemann, and M. Sachwitz, Phys.Lett. **B206**, 539 (1988).
- [22] R. G. Stuart, Phys.Lett. **B262**, 113 (1991).
- [23] R. G. Stuart, Phys.Lett. **B272**, 353 (1991).
- [24] S. Dittmaier *et al.*, (2012), 1201.3084.
- [25] C. Anastasiou, S. Buehler, F. Herzog, and A. Lazopoulos, JHEP **1204**, 004 (2012), 1202.3638.

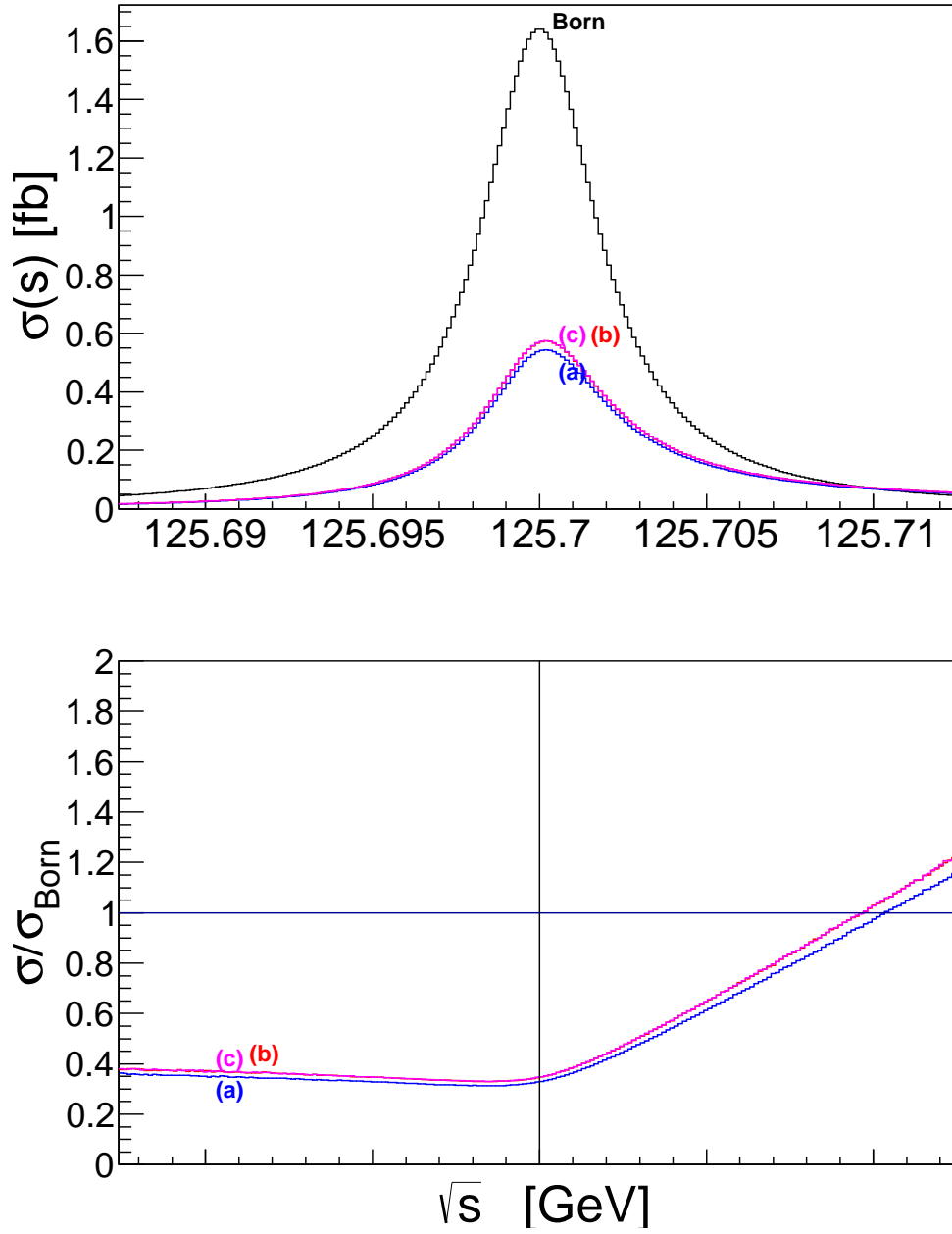


Figure 1: Study of the pure QED effect in the Higgs line-shape for electron collider. The plots show Born cross sections of eq. (2.1) and cross section affected by QED ISR, following eq. (2.2) for three types $I = a, b, c$ of the QED radiator functions defined in eq. (2.3). The ratios with respect to Born cross section are also shown.

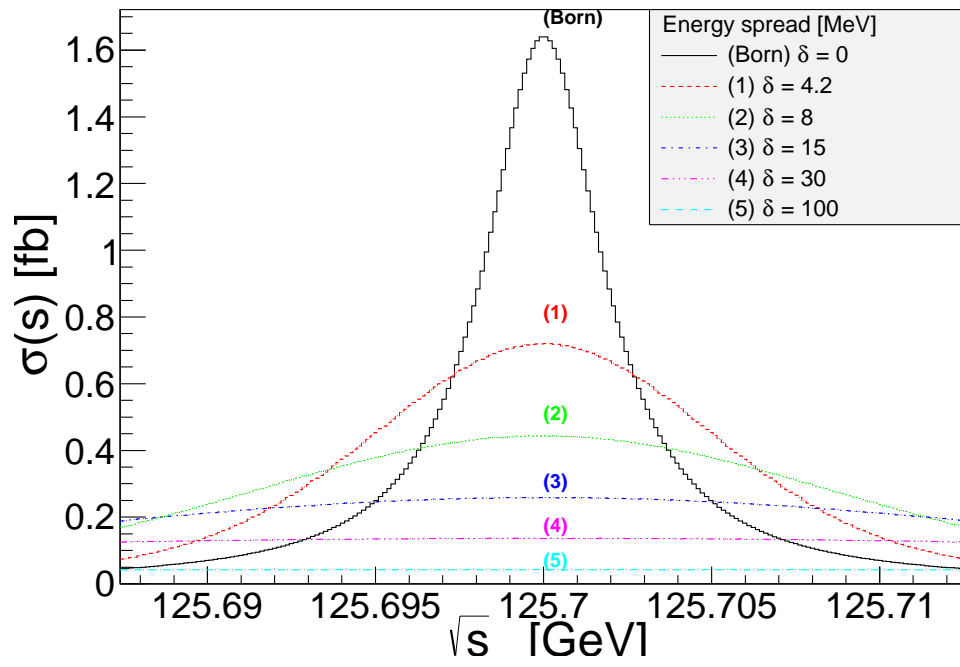


Figure 2: Higgs production cross section in the electron-positron collider for several values of the machine energy spread $\delta = 0, 4.2, 8, 15, 30, 100$ MeV. The QED ISR effect is not included.

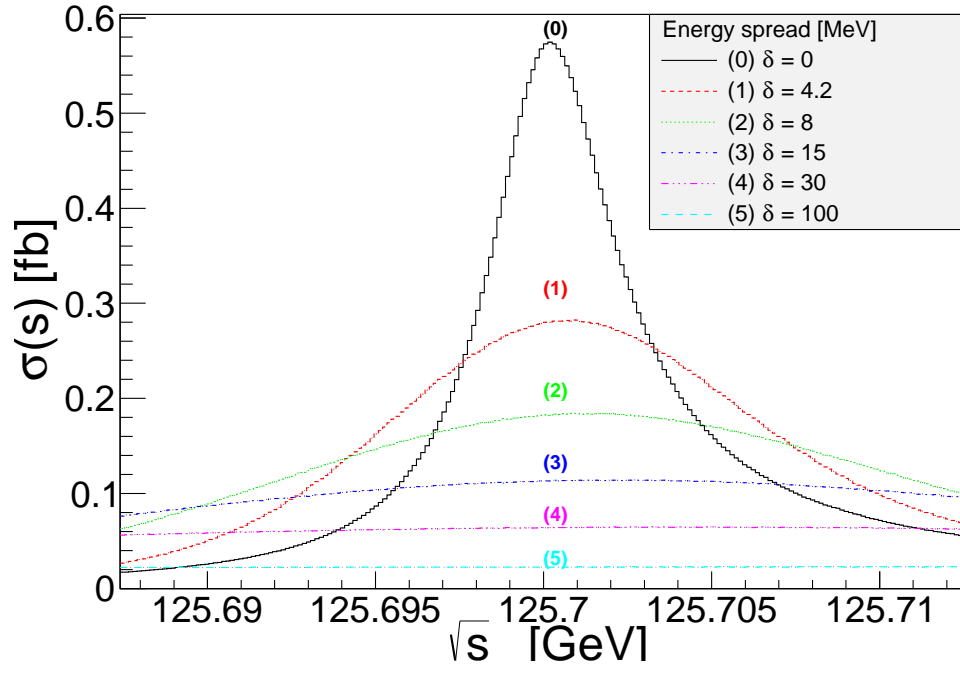


Figure 3: Higgs production cross section in the electron-positron collider for several values of the machine energy spread $\delta = 0, 4.2, 8, 15, 30, 100$ MeV. The QED ISR effect is included according to eq. (3.3), for ISR type (c).

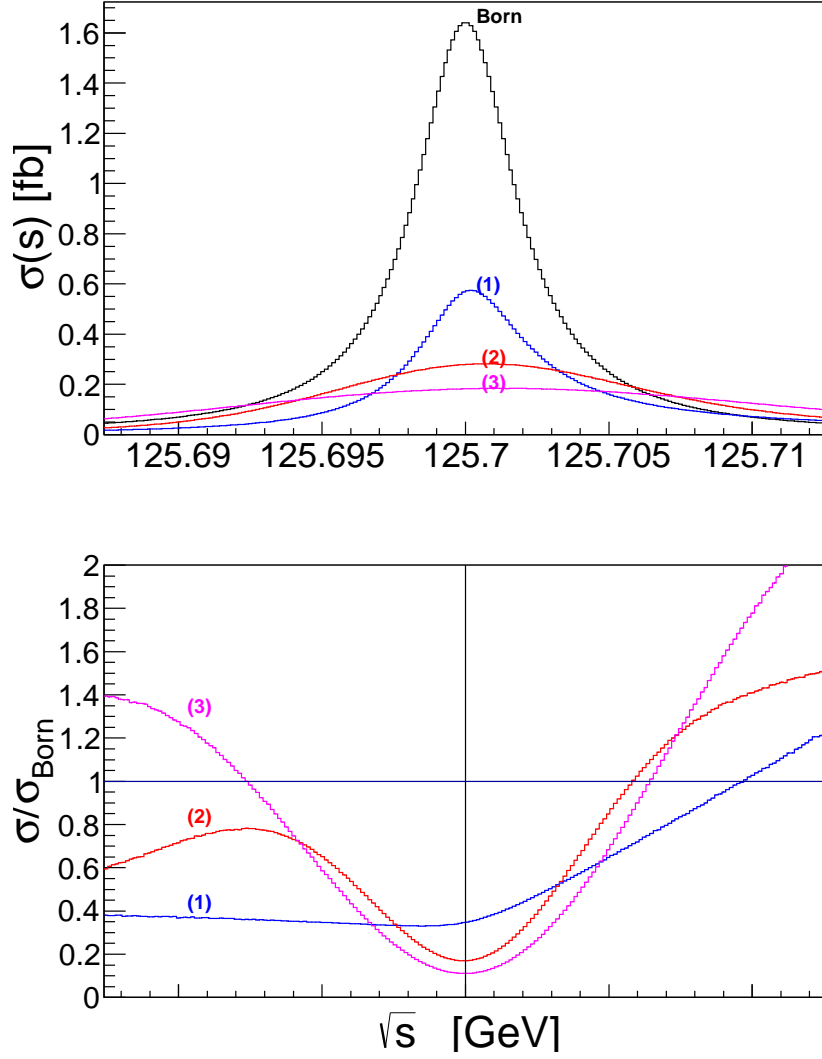


Figure 4: Line-shape of the direct Higgs production process in the electro-positron collider including effect of ISR type (c) and the machine energy spread. No energy spread is included (only ISR is on) in the line marked with (1), while lines marked with (2) and (3) include ISR and energy spread $\delta = 4.2$ MeV and $\delta = 8.0$ MeV according to eq. (3.3). Reference Born cross section is also shown and the ratios with respect to Born are also plotted.

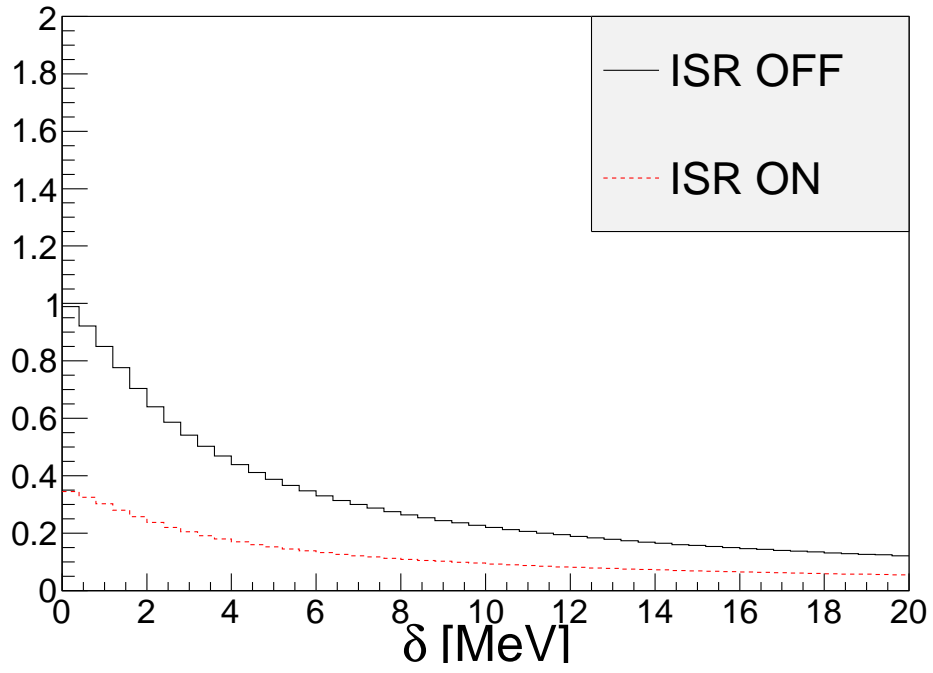


Figure 5: The dependence of the Higgs production process at the resonance peak, $E = M_H$ in the electron-positron collider on the energy spread δ , divided by the Born cross section, for QED ISR switched on and off.

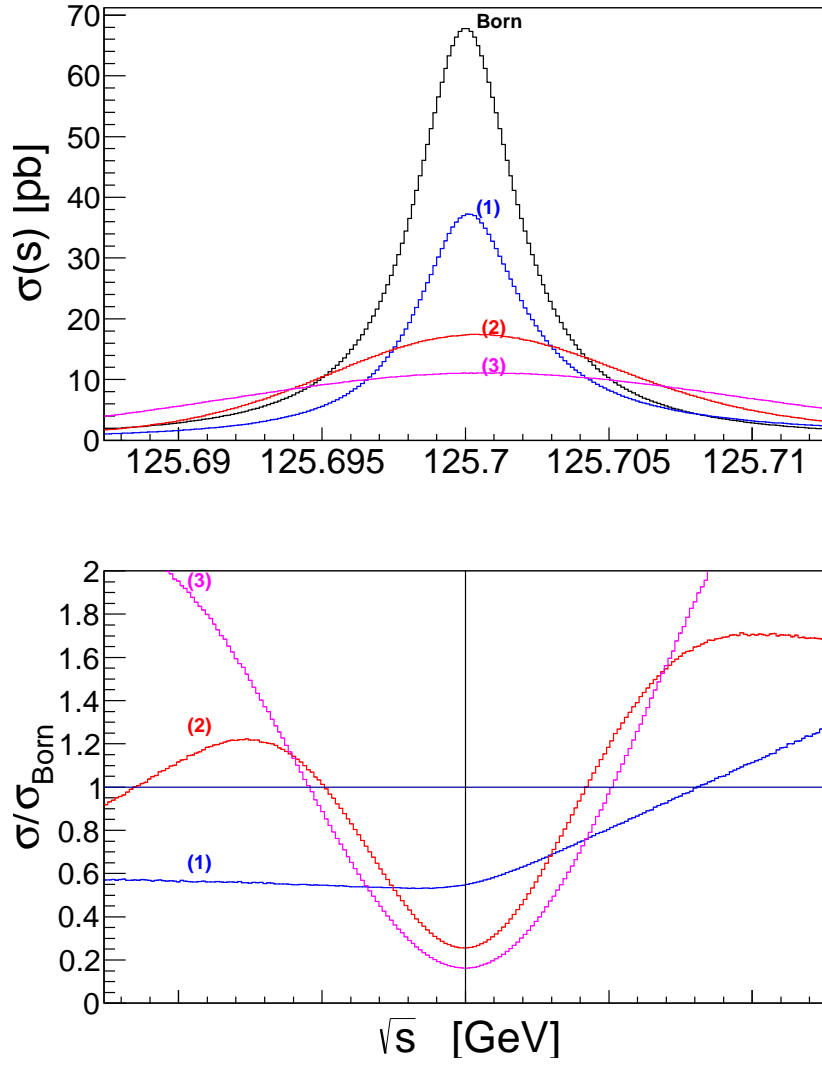


Figure 6: Line-shape of the direct Higgs production process in the $\mu^+\mu^-$ collider including effect of ISR type and the machine energy spread. The same input and notation as in Fig. 4

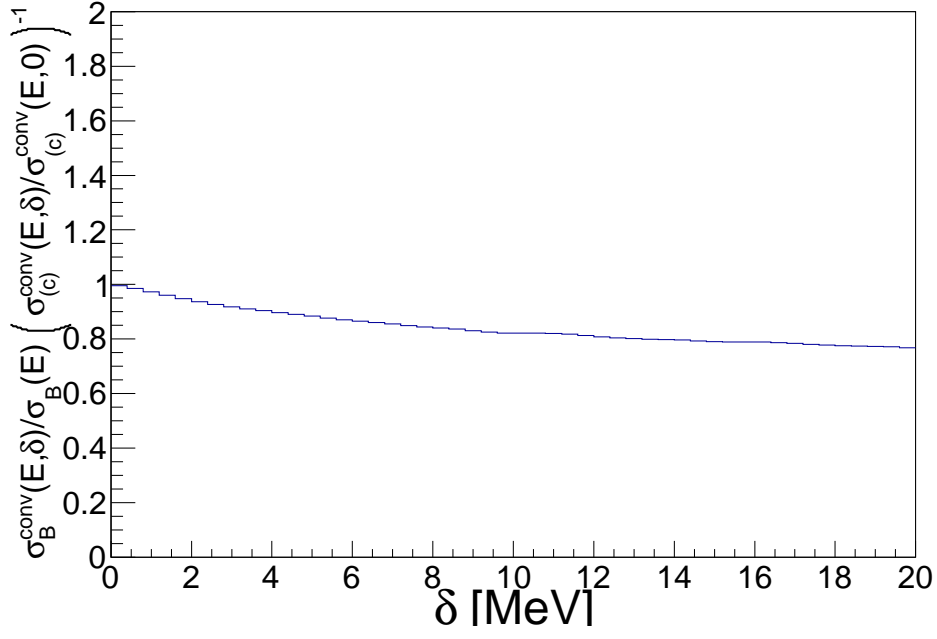


Figure 7: Numerical cross-check of the validity of the approximation shown in eq. (4.2) for $E = M_H$.